iScience

CellPress
OPEN ACCESS

Article

Swine acute diarrhea syndrome coronavirus induces autophagy to promote its replication via the Akt/mTOR pathway

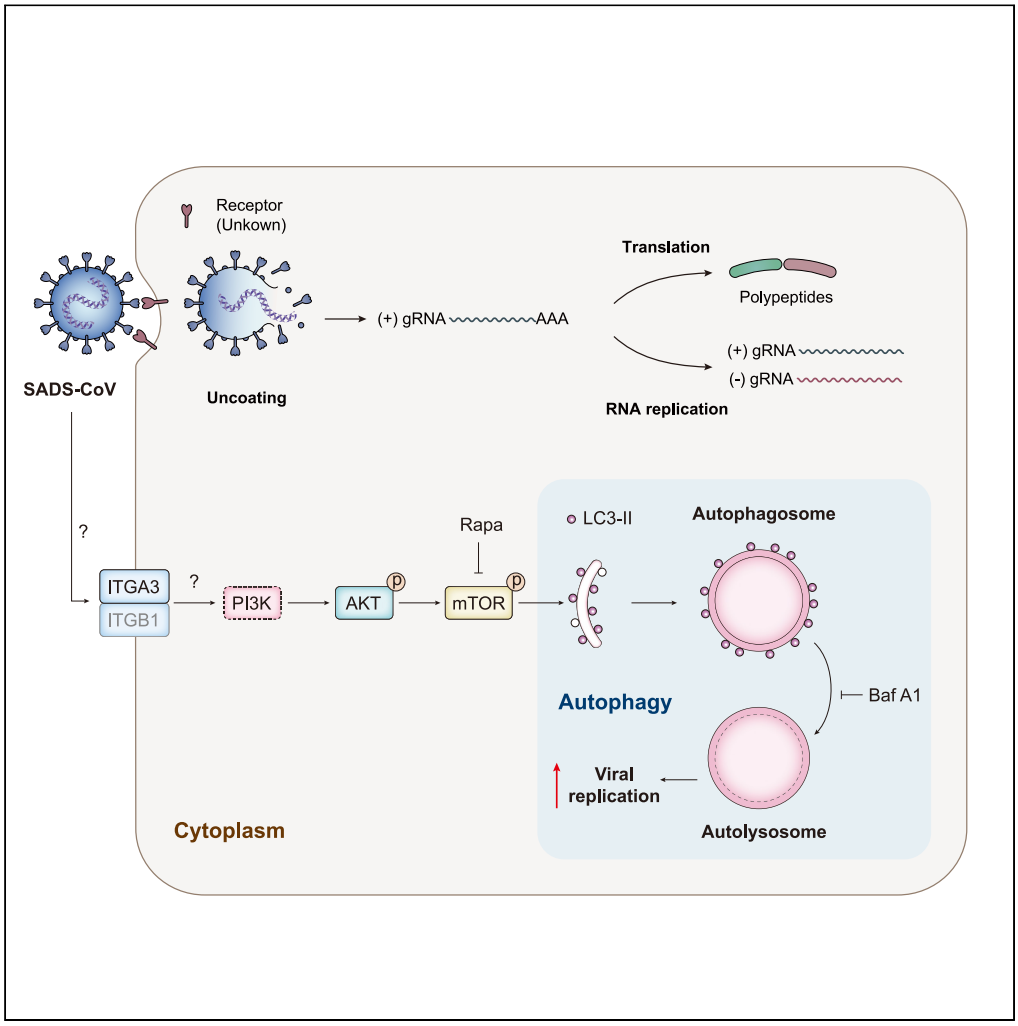

Siying Zeng, Yan Zhao, Ouyang Peng, ..., Chunyi Xue, Yongchang Cao, Hao Zhang

zhanghao5@mail.sysu.edu.cn

Highlights

SADS-CoV triggers autophagy pathway to facilitate its proliferation

Inhibition of autophagy flux impairs SADS-CoV replication

SADS-CoV negatively regulates Akt/mTOR pathway to induce autophagy

ITGA3 prevents SADS-CoV production through autophagy inhibition

Zeng et al., iScience 25, 105394
November 18, 2022
https://doi.org/10.1016/j.isci.2022.105394

iScience

CellPress
OPEN ACCESS

Article

Swine acute diarrhea syndrome coronavirus induces autophagy to promote its replication via the Akt/mTOR pathway

Siying Zeng,[1] Yan Zhao,[1] Ouyang Peng,[1] Yu Xia,[1] Qiuping Xu,[2,3] Hongmei Li,[4] Chunyi Xue,[1] Yongchang Cao,[1] and Hao Zhang[1,5,*]

SUMMARY

Swine acute diarrhea syndrome coronavirus (SADS-CoV) is an enveloped, single-stranded, positive-sense RNA virus belonging to the Coronaviridae family. Increasingly studies have demonstrated that viruses could utilize autophagy to promote their own replication. However, the relationship between SADS-CoV and autophagy remains unknown. Here, we reported that SADS-CoV infection-induced autophagy and pharmacologically increased autophagy were conducive to viral proliferation. Conversely, suppression of autophagy by pharmacological inhibitors or knockdown of autophagy-related protein impeded viral replication. Furthermore, we demonstrated the underlying mechanism by which SADS-CoV triggered autophagy through the inactivation of the Akt/mTOR pathway. Importantly, we identified integrin α3 (ITGA3) as a potential antiviral target upstream of Akt/mTOR and autophagy pathways. Knockdown of ITGA3 enhanced autophagy and consequently increased the replication of SADS-CoV. Collectively, our studies revealed a novel mechanism that SADS-CoV-induced autophagy to facilitate its proliferation via Akt/mTOR pathway and found that ITGA3 was an effective antiviral factor for suppressing viral infection.

INTRODUCTION

Coronaviruses are a large group of enveloped, single-stranded, positive-sense RNA viruses with strong recombination tendency and high mutation rates (Herrewegh et al., 1998; Woo et al., 2006). In the first two decades of this century, three highly pathogenic zoonotic coronaviruses, including severe acute respiratory syndrome coronavirus (SARS-CoV), Middle East respiratory syndrome coronavirus (MERS-CoV), and the ongoing SARS-CoV-2, have caused widespread human infection (Corman et al., 2012; Drosten et al., 2003; Zhou et al., 2020). These three viruses are thought to originate from bat species and intermediate mammalian hosts with the ability to cross the species barrier and zoonotic transmission (Millet et al., 2021). In addition, a recent study reported for the first time that porcine deltacoronavirus (PDCoV) can also infect humans, highlighting that more attention should be paid to poultry and livestock coronaviruses with a board host spectrum (Lednicky et al., 2021). Swine acute diarrhea syndrome coronavirus (SADS-CoV) is another recently emerged coronavirus discovered in 2017, (Gong et al., 2017; Pan et al., 2017; Zhou et al., 2018) which was also identified as an HKU2-related coronavirus with a bat-origin (Gong et al., 2017; Zhou et al., 2018). Moreover, several recent studies have shown that SADS-CoV has a wide range of cell tropism, which can infect cells not only from natural host pigs, but also from rats, monkeys, and humans (Yang et al., 2019b; Edwards et al., 2020; Luo et al., 2021). These data highlight the potential cross-species transmissibility of SADS-CoV, and therefore, a more comprehensive understanding of the interaction between host and pathogen is needed to promote the development of novel antiviral therapies for the prevention and control.

Autophagy is an evolutionarily conserved degradative biological process that is important in maintaining cellular homeostasis by eliminating damaged organelles and long-lived proteins (Mizushima, 2009). It can be activated by many intracellular and extracellular stresses, such as cellular starvation, growth factor depletion, organelle damage, endoplasmic reticulum stress, and viral infection (King et al., 2011; Kroemer et al., 2010; Mizushima et al., 2010; Sun et al., 2018). In the process of autophagy, the phagophore, a cup-shaped isolation membrane, nucleates and elongates to engulf intracellular cargo, and then sequesters the

[1]State Key Laboratory of Biocontrol, School of Life Sciences, Sun Yat-sen University, Guangzhou 510006, China

[2]Guangdong Provincial Key Laboratory of Malignant Tumor Epigenetics and Gene Regulation, Sun Yat-sen Memorial Hospital, Sun Yat-sen University, Guangzhou 510120, China

[3]Medical Research Center, Sun Yat-sen Memorial Hospital, Sun Yat-sen University, Guangzhou 510120, China

[4]School of Life Sciences, Sun Yat-sen University, Guangzhou 510006, China

[5]Lead contact

*Correspondence: zhanghao5@mail.sysu.edu.cn

https://doi.org/10.1016/j.isci.2022.105394

contents in a double-membraned autophagosome, which fuses with late endosomes for degradation (Boya et al., 2013; Yang and Klionsky, 2009). The microtubule-associated protein light chain 3 (LC3), encoded by the mammalian homolog of autophagy-related gene (ATG) 8, plays a key role in the maturation of the phagophore. During this stage, cytosolic LC3-I is covalently linked to phosphatidylethanolamine (PE) and converts into an active, autophagosome membrane-bound, phosphatidylethanolamine conjugated form, LC3-II. The increased synthesis and processing of LC3 make it a hallmark of autophagy and an indicator of autophagy activity (Barth et al., 2010).

As an important part of the host defense against virus infection, the activation of autophagy leads to the isolation of subviral components in autophagosomes for lysosomal degradation, a process known as xenophagy or virophagy (Dong and Levine, 2013). However, studies on the interaction between autophagy and viruses revealed that some viruses, such as herpes simplex virus type 2 (HSV2), human papillomavirus, and Zika Virus, have evolved strategies to block autophagy and evade subsequent degradation, while therapeutic enhancement of autophagy can decrease viral burden and improve cells survival (Hait et al., 2020; Jia et al., 2016; Mattoscio et al., 2018; Sahoo et al., 2020). In some cases, viruses could hijack the autophagy pathway for their own proliferation (Dreux and Chisari, 2010; Richards and Jackson, 2013; Sumpter and Levine, 2011). For instance, some RNA viruses, such as coxsackievirus, Influenza A Virus, and hepatitis C virus (HCV), seem to induce the formation of double-membrane compartments as a physical platform for the viral replication machinery (Wang et al., 2019b; Ke and Chen, 2011a; Mohamud et al., 2018). Most coronaviruses (CoVs), including SARS-CoV, SARS-CoV-2, and porcine epidemic diarrhea virus (PEDV), also induce autophagy, and the endoplasmic reticulum (ER)-derived double-membrane vesicles (DMVs) are considered to be the site of viral transcription-replication complex assembly, which indicates that coronaviruses are likely to mimic the cellular autophagy pathway (Angelini et al., 2013; Guo et al., 2017; Hui et al., 2021; Snijder et al., 2020). In addition, individual components of the autophagic machinery could be utilized, independent of their activity in autophagic processing. It has been found that the canonical autophagic pathway is not necessary for mouse hepatitis virus (MHV) infection, but the non-lipidized form of LC3-I is associated with coronavirus-induced DMV and is required for MHV replication (Reggiori et al., 2010).

Of note, a serine/threonine kinase called the mechanistic target of rapamycin (mTOR), is a major player in integrating metabolic, growth factor, and energy signals into the autophagy pathway (Diaz-Troya et al., 2008). mTOR negatively regulates autophagy via modulating autophagy-related proteins and lysosome biosynthesis (Wang et al., 2019a). Upstream of mTOR, the phosphoinositide 3-kinase (PI3K)/the serine-threonine kinase Akt pathway is one of the critical signal cascades regulating its activity, which also plays a key role in coordinating cellular responses to a variety of internal and external stimuli (Manning and Toker, 2017). Activation of the PI3K-Akt-mTOR pathway inhibits autophagy through mTOR phosphorylation (He and Klionsky, 2009), whereas signaling loss eliminates the negative regulation of mTOR and, consequently, some viruses may usurp these cascades to facilitate viral replication. In support of this, several research have demonstrated that viruses such as coxsackievirus (Chang et al., 2017), avian influenza A virus (Ma et al., 2011), and Zika virus (Liang et al., 2016), could modulate the PI3K-Akt-mTOR pathway, thereby hijacking autophagy for survival.

In the present study, we reported that SADS-CoV infection-induced autophagy both in African green monkey kidney (Vero E6) cells and porcine ileum epithelial cell line (IPI-FX). Importantly, induction or inhibition of autophagy via pharmacological treatment could promote/reduce the viral replication, respectively, suggesting that SADS-CoV hijacked the autophagy pathway for proliferation during the viral invasion. Based on the previous work of transcriptome (Zeng et al., 2021), we intended to explore the mechanism of virus-induced autophagy and found that SADS-CoV could activate autophagy by suppressing the Akt/mTOR signaling pathway. Further screening of proteomic research revealed that integrin α3 (ITGA3) could be a potential functional protein as it was significantly reduced in SADS-CoV-infected Vero E6 cells. Exogenous expression and RNA interference suggested that ITGA3 plays an antiviral role by inhibiting autophagy; moreover, this suppression could be mediated by Akt/mTOR pathway. Taken together, our findings identified a novel antiviral target of SADS-CoV, which could affect viral replication via the regulation of the autophagy pathway.

RESULTS

Swine acute diarrhea syndrome coronavirus infection activates the autophagy pathway

To explore the relationship between SADS-CoV infection and autophagy, we first determined whether SADS-CoV infection could induce autophagy in Vero E6 cells and IPI-FX cells by Western blotting. Since

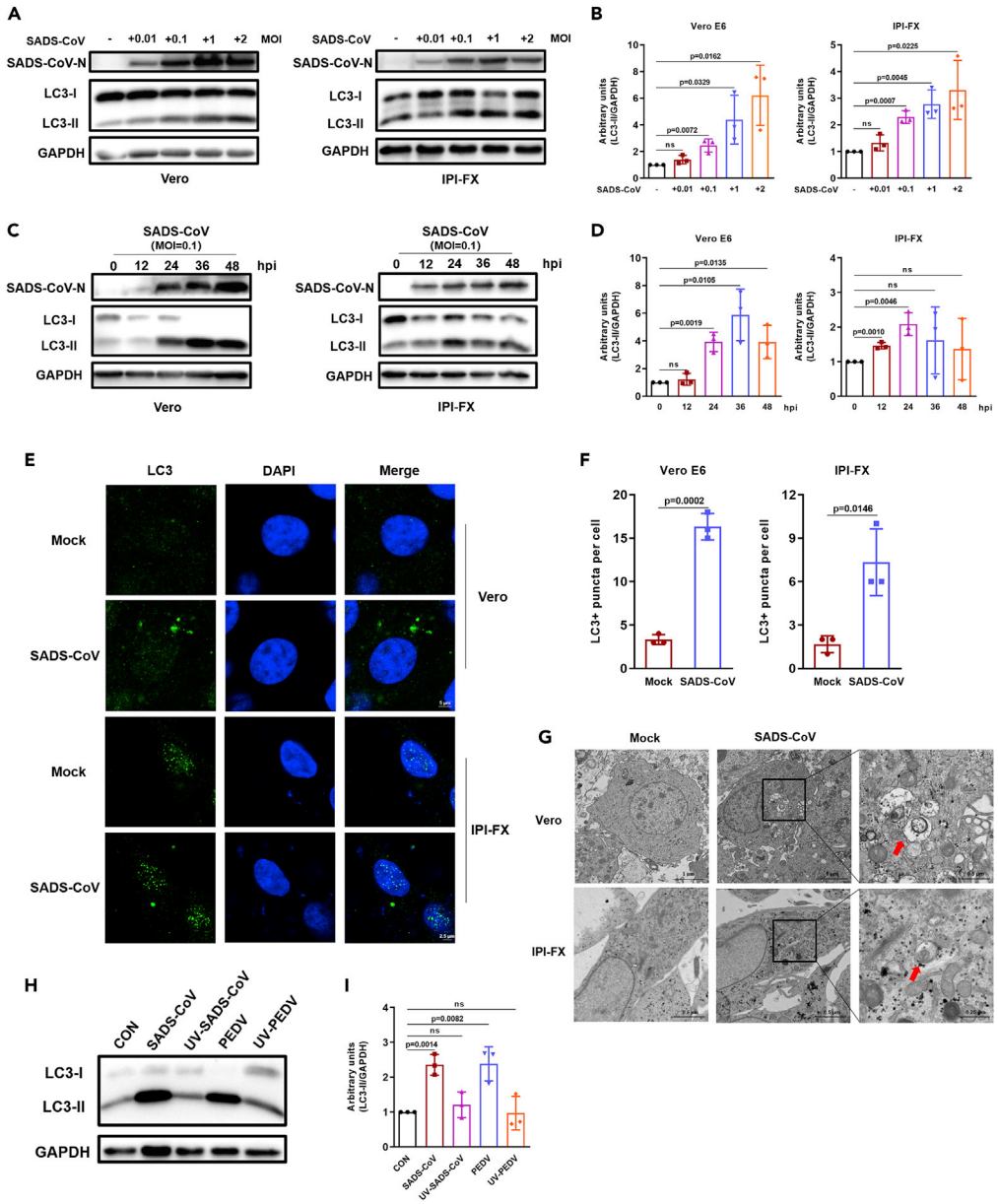

Figure 1. SADS-CoV infection triggers the autophagy pathway

(A) Vero E6 cells and IPI-FX cells were mock infected or infected with SADS-CoV at different MOI (0.01, 0.1, 1, and 2). Cell lysates were collected at 24 hpi and subjected to Western blot analysis.

(B) The normalized ratios of LC3-II/GAPDH at different MOI were quantified and plotted.

(C) Vero E6 cells and IPI-FX cells were infected with SADS-CoV at an MOI of 0.1. Cell lysates were harvested at 0, 12, 24, 36, and 48 hpi, and processed for Western blot analysis.

(D) The normalized ratios of LC3-II/GAPDH at different time points were quantified and plotted.

(E) Vero E6 cells and IPI-FX cells were mock infected or infected with SADS-CoV at an MOI of 0.1. Then, cells were fixed at 24 hpi and subjected to the immunoconfocal microscopy analysis to detect LC3 puncta (green). The nuclei were stained with DAPI (blue). Scale bar, 5 μm in Vero E6 cells, 2.5 μm in IPI-FX cells.

(F) The number of LC3 puncta per cell was counted from confocal images.

(G) Vero E6 cells and IPI-FX cells were treated as described in the legend of Figure 1E and subjected to transmission electron microcopy. Magnified views of the autophagosome-like vesicles are enclosed by black square frames. Scale bar, 0.5 μm in Vero E6 cells, 0.25 μm in IPI-FX cells.

Figure 1. *Continued*

(H) Vero E6 cells were infected with replication-competent or UV-inactivated SADS-CoV (MOI = 0.1) for 24 h. Cell samples were processed for western blot analysis. PEDV and UV-inactivated PEDV were used as positive control and negative control, respectively.

(I) The normalized ratios of LC3-II/GAPDH were calculated to present the autophagic level. The data presented are means ± SD from at least three independent experiments. ns, non-significant.

the ratio of expression level between LC3-II, a hallmark of autophagosome, and housekeeping gene expression is considered to be an accurate indicator of autophagic activity, we evaluated the density ratio of LC3-II to GAPDH. The expression level of LC3-II has significantly increased in SADS-CoV infected cells with different MOI from 0.1 to 2, but there was little change in low-dose 0.01 MOI compared to control cells (Figures 1A and 1B). In addition, we detected the autophagic activity at different time points (0, 12, 24, 36, 48 h of infection) during viral infection with an MOI of 0.1 and found that the expression of LC3-II was increased with the course of infection, while the highest expression level occurred at 36 h post-infection (hpi) and 24 hpi in Vero E6 cells and IPI-FX cells, respectively (Figures 1C and 1D). To further confirm the accumulation of autophagosome, confocal microscopy and transmission electron microcopy (TEM) were performed (Figures 1E-1G) both in Vero E6 cells and IPI-FX cells. Indeed, we observed increased formation of LC3 puncta and autophagosomes in infected cells.

In order to investigate whether SADS-CoV-induced autophagy requires viral replication, LC3-II expression was measured in Vero E6 cells upon ultraviolet (UV)-inactivated SADS-CoV infection. PEDV was used as a control, for it was reported that autophagy could be triggered by active but not ultraviolet (UV)-inactivated PEDV (Guo et al., 2017). Before the experiment, the infectivity of UV-inactivated viruses was detected by $TCID_{50}$ and real-time fluorescence quantitative PCR (qPCR) assay (data not shown). The results showed that neither the UV-inactivated SADS-CoV nor UV-inactivated PEDV did not stimulate the expression level of LC3-II relative to mock-treated cells, while native SADS-CoV and PEDV normally induced autophagy (Figures 1H and 1I). Altogether, these results indicate that SADS-CoV infection induces the autophagy pathway and this activation requires the replication of native virions.

Swine acute diarrhea syndrome coronavirus-induced autophagy is conducive to viral replication

To determine the role of autophagy in SADS-CoV replication, we used well-established autophagy regulators to trigger or suppress the autophagy pathway and then checked their effects on viral replication by Western blotting. All drugs or compounds (including those mentioned later in discussion) were pretested for toxicity at the concentration used and the results showed no significant effect on cell activity (Figure S1). Pharmacological treatment of rapamycin, an inducer of autophagy, was added into the Vero E6 cells and IPI-FX cells followed the infection of SADS-CoV at an MOI of 0.1, then cell lysates were harvested at 24 and 36 h post-transfection (hpi). As expected, the LC3-II expression level was increased in rapamycin-treated cells and importantly, the expression level of nucleocapsid protein (N) of SADS-CoV was also upregulated (Figures 2A and 2B). In contrast, cells treated with autophagy inhibitor 3-methylademine (3-MA) in a similar way resulted in decreased expression of LC3-II and N protein relative to non-treated infected cells (Figures 2C and 2D). To further confirm that autophagy modulation was able to influence viral infection, $TCID_{50}$ was performed to assess viral load under the different conditions tested (Figure 2E). A similar pattern of changes in viral titers was also observed both in Vero E6 cells and IPI-FX cells. These substantial evidence reveal that SADS-CoV utilizes the autophagy pathway to favor its replication during viral infection.

Swine acute diarrhea syndrome coronavirus infection induces complete autophagy flux

With the progress of the autophagy pathway, autophagosome fuses with lysosomes, and subsequently leading to the degradation of autophagosome cargo. It is thought that some coronaviruses may allow or promote the fusion of the autophagosome with the late endosome for survival (van der Meer et al., 1999), while in some cases, coronaviruses disrupt the fusion of the autophagosome with the lysosome and thus block the autophagic flux (Oudshoorn et al., 2017). Given that sequestosome 1 (SQSTM1) is degraded within autolysosomes, it is widely considered a marker for monitoring autophagic flux. Therefore, to further decipher the functional autophagy activity during SADS-CoV infection, we investigated the level of SQSTM1 in Vero E6 cells at 24 and 36 hpi. Compared with uninfected control cells, SQSTM1 showed a significant decrease upon viral infection, suggesting that the autophagy pathway

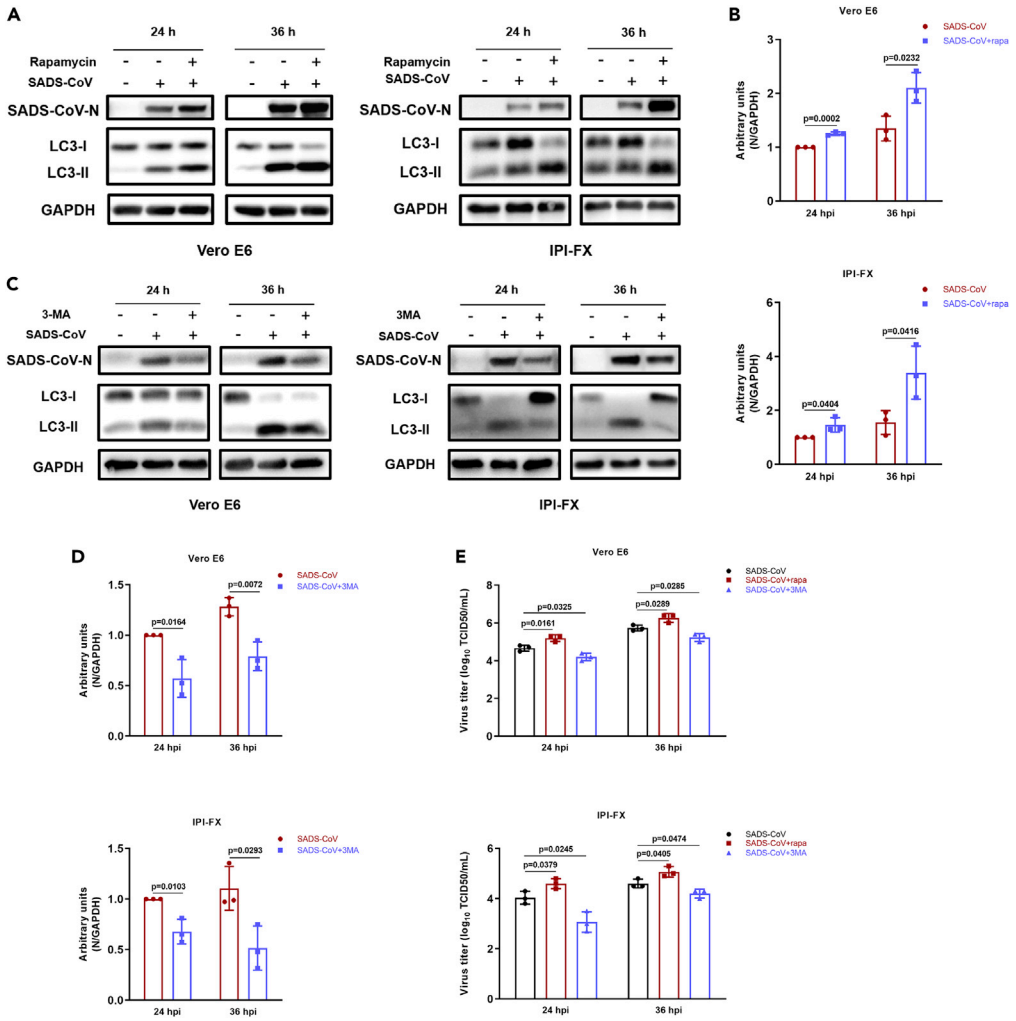

Figure 2. The autophagy machinery is required for SADS-CoV production

(A and C) Vero E6 cells and IPI-FX cells were mock infected or infected with SADS-CoV (MOI = 0.1) and then treated with rapamycin or 3-MA at 6 hpi. Cell samples were collected at 24 and 36 hpi. The effect of rapamycin or 3-MA on the level of autophagy and the replication of SADS-CoV were tested by Western blot analysis.

(B and D) The normalized ratios of SADS-CoV-N/GAPDH under rapamycin or 3-MA condition.

(E) The viral titer of the culture supernatant was determined by $TCID_{50}$. The data presented are means ± SD from at least three independent experiments.

was functionally active (Figures 3A and 3B). We suspected that SADS-CoV-induced complete autophagy flux which was required for virus replication. To corroborate our hypothesis, the cells were infected with SADS-CoV and subsequently subjected to the treatment of bafilomycin A1 (Baf A1), an inhibitor of autophagosome-lysosome fusion. The quantities of LC3-II and SQSTM1 were upregulated in Baf A1 treatment infected cells due to the reduction of autophagic flux and accumulation of autophagosome, and as expected, the expression of N protein was suppressed (Figures 3C and 3D). Similar results were obtained in viral titers that Baf A1-treated cells showed a lower viral load than untreated cells at 24 and 36 hpi (Figure 3E). Confocal microscopy was performed as an additional assay to visualize the autophagic structures and the virions under Baf A1 conditions, and the images showed an increase in the formation of LC3 puncta but a decrease in N protein level (Figure 3F). Notably, we equally noticed that there were fewer red immunostainings of viruses where LC3 puncta accumulated in large quantities in Baf A1-treated cells. The observation reinforced our previous results that complete autophagy flux was required for SADS-CoV replication while blocking the fusion of the autophagosome with the lysosome impeded viral proliferation.

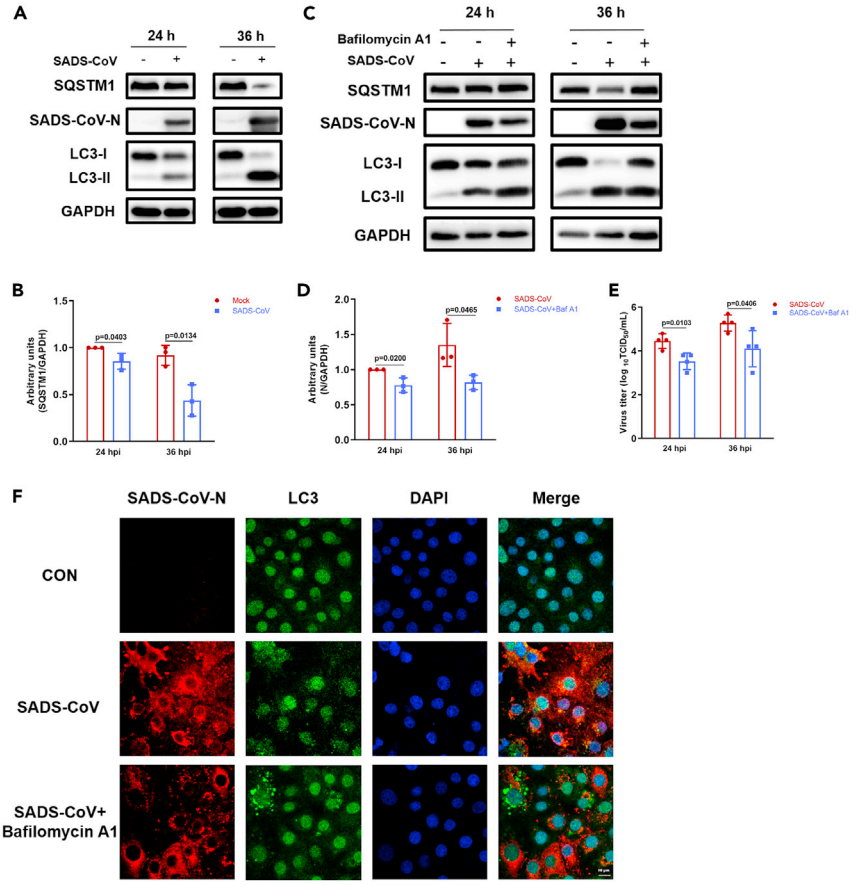

Figure 3. SADS-CoV replication requires autophagy flux

(A) Vero E6 cells were mock infected or infected with SADS-CoV at 0.1 MOI. Cell lysates were collected and subjected to western blot analysis at 24 and 36 hpi.

(B) The normalized ratios of SQSTM1/GAPDH were calculated to present functional autophagy activity.

(C) Vero E6 cells were mock infected or infected with SADS-CoV (MOI = 0.1) and then treated with bafilomycin A1 at 6 hpi. Cell samples were collected at 24 and 36 hpi. The effect of bafilomycin A1 on the level of autophagy activity and the replication of SADS-CoV were tested by western blot analysis.

(D) The normalized ratios of SADS-CoV-N/GAPDH under bafilomycin A1 condition were quantified and plotted.

(E) The viral titer of the culture supernatant was determined by TCID50.

(F) Infected Vero E6 cells (MOI = 0.1) were treated with bafilomycin A1 at 6 hpi and were fixed at 24 hpi. Confocal microscopy was performed to assess the effect of bafilomycin A1 on the autophagy flux and viral replication. Scale bar, 10 μm. The data presented are means ± SD from at least three independent experiments.

Knockdown of the endogenous autophagy-related gene 5 reduces Swine acute diarrhea syndrome coronavirus replication

The biogenesis of autophagy requires the interaction of various autophagy-related proteins, among which ATG5 is an essential protein for autophagosome formation (Mizushima et al., 2001). Consistently, ATG5 was upregulated in a pattern similar to LC3-II in Vero E6 cells during SADS-CoV infection (Figures 4A and 4B). To further validate the relationship between autophagy and SADS-CoV proliferation, we extended the above research by further analyzing the effects of endogenous ATG5 knockdown on viral replication through target-specific RNA interference. We searched for two small interfering RNAs (siRNA) targeting ATG5 (siATG5) and detected their knockdown efficiency at 48 h post-transfection in Vero E6 cells by Western blotting. All the cells transfected with siATG5 displayed significant reductions in ATG5 protein expression (Figure 4C) compared to negative control (NC) cells. Subsequently, Vero E6 cells were infected with SADS-CoV after the transfection of siNC or siATG5 for 24 h, and the cell lysates were collected at 24 hpi. Western blot analysis showed that ATG5 silencing led to a suppression of LC3 turnover, accompanied by a reduction in the synthesis of viral N protein (Figures 4D and 4E). Likewise, viral titration validated

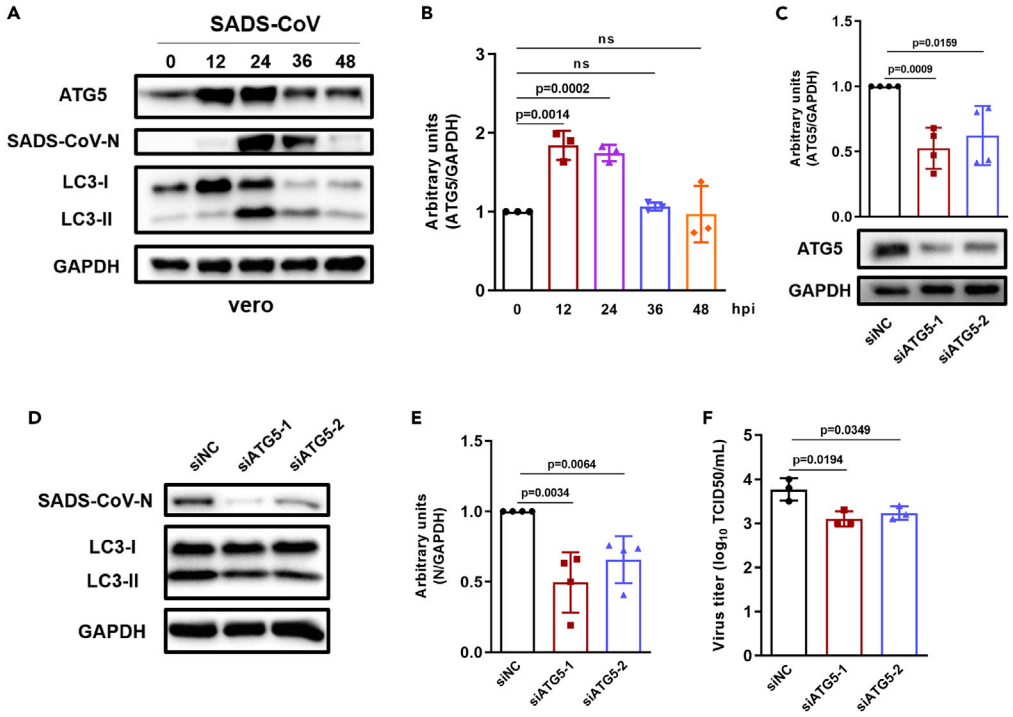

Figure 4. Silencing ATG5 gene reduces the SADS-CoV titer

(A) Vero E6 cells were infected with SADS-CoV at an MOI of 0.1. Cell lysates were harvested at 0, 12, 24, 36, and 48 hpi, and processed for Western blot analysis.

(B) The normalized ratios of ATG5/GAPDH at different time points were quantified and plotted.

(C) Vero E6 cells were transfected with siATG5 or siNC and were collected for Western blot analysis at 48 hpi. Knockdown efficiency of specific siRNA was determined by the relative expression of ATG5 to GAPDH.

(D) Vero E6 cells treated with the indicated siRNAs were infected with SADS-CoV at an MOI of 0.1 after 24 h transfection. Then the cells were harvested at 24 hpi and subjected to Western blot analysis.

(E) The normalized ratios of SADS-CoV-N/GAPDH were calculated to reflect the effect of ATG5 knockdown on the viral replication.

(F) The viral titer of the culture supernatant was measured by $TCID_{50}$. The data presented are means ± SD from at least three independent experiments. ns, non-significant.

that cells transfected with siATG5 exhibited a decrease in viral yields relative to the control (Figure 4F). Taken together, these findings suggest that SADS-CoV-induced autophagy is ATG5 dependent, and knockdown of the endogenous ATG5 could thwart SADS-CoV replication.

Swine acute diarrhea syndrome coronavirus induces autophagy via the Akt/mTOR pathway

Autophagy is modulated by a variety of cellular signaling pathways, in which the mTOR pathway plays a key role in autophagy initiation. Upstream of mTOR, Akt kinase activity is a very important regulatory factor. The transcriptome of Vero E6 cells infected with SADS-CoV in our previous studies implied that Akt/mTOR pathway might act as a role in viral infection (Zeng et al., 2021). Therefore, we hypothesized that SADS-CoV-induced cellular autophagy via the Akt/mTOR signal cascade. To investigate the effect of SADS-CoV infection on Akt/mTOR signaling, we first monitored the status of Akt and mTOR activation in Vero E6 cells at different time points (0, 12, 24, 36 and 48 h) during SADS-CoV infection by determining the levels of total protein and phosphorylation. Our results showed no significant changes in the levels of total Akt and mTOR, but the phosphorylation of both proteins was time-dependently downregulated (Figures 5A and 5B). Meanwhile, the observation of increased LC3 conversion upon infection was consistent with that Akt/mTOR signaling is inversely correlated with autophagy induction.

To further examine the relationship between SADS-CoV proliferation and Akt/mTOR pathway, pharmacological modulators of Akt activity were employed in infected cells and subjected to western blot analysis at 24 hpi. Treatment of an allosteric small-molecule inhibitor of Akt MK2206 led to the reduction of Akt

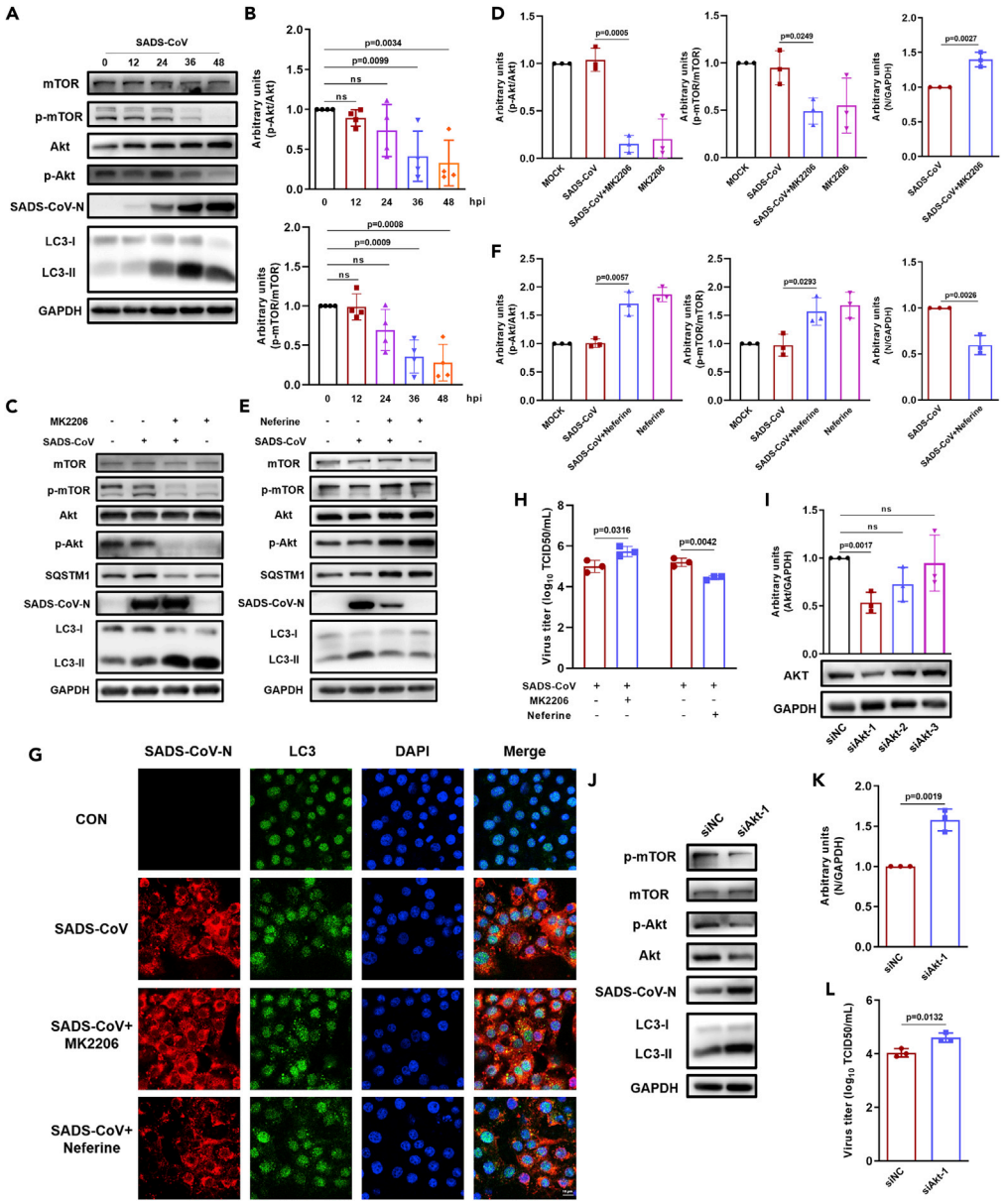

Figure 5. SADS-CoV infection inhibits the Akt/mTOR signaling pathway to induce autophagy

(A) Vero E6 cells were infected with SADS-CoV at an MOI of 0.1. Cell samples were collected at various time points and subjected to immunoblot with indicated antibodies.

(B) The normalized ratios of p-Akt/Akt and p-mTOR/mTOR, respectively, were quantified and plotted.

(C and E) Vero E6 cells were mock infected or infected with SADS-CoV (MOI = 0.1) and then treated with MK2206 or Neferine at 1.5 hpi. Cell samples were collected at 24 hpi. The effect of the regulators on the level of Akt and mTOR activities and the replication of SADS-CoV were measured with indicated antibodies.

(D and F) The normalized ratios of N/GAPDH, p-Akt/Akt, and p-mTOR/mTOR under different conditions were quantified and plotted. (G) Vero E6 cells were prepared as described in the legend of Figures 5C and 5E. Confocal microscopy was performed to examine the effect of MK2206 or Neferine on autophagy activity and viral replication. Scale bar, 10 μm.

(H) The viral titer of the culture supernatant was determined by $TCID_{50}$.

(I) Vero E6 cells were transfected with siAkt or siNC and were harvested for Western blot analysis at 48 hpi. Knockdown efficiency was tested by the relative expression of Akt to GAPDH.

(J) Vero E6 cells treated with the indicated siRNAs were infected with SADS-CoV at an MOI of 0.1 after 24 h transfection. Then the cells were harvested at 24 hpi and subjected to Western blot analysis.

(K) The normalized ratios of SADS-CoV-N/GAPDH in different transfected cells.

(L) The viral titer of the culture supernatant was determined by $TCID_{50}$. The data presented are means ± SD from at least three independent experiments. ns, non-significant.

phosphorylation, which subsequently resulted in the suppression of mTOR phosphorylation. Compared with the control cells, inhibition of Akt/mTOR signal cascade upregulated the expression level of LC3-II, indicating a higher level of autophagy, and as a consequence, viral N protein was enhanced (Figures 5C and 5D). In addition, we treated Vero E6 cells with another Akt regulator Neferine, which in previous studies has been shown to prevent autophagy through the activation of the Akt/mTOR pathway in muscle cells (Baskaran et al., 2016), to make our assessment of the role of Akt/mTOR more credible. As expected, Neferine-treated cells possessed a higher level of phosphorylation in Akt and mTOR, and a lower efficiency of LC3 turnover (Figures 5E and 5F). Certainly, the expression of SADS-CoV N protein was restrained. We also visualized the differential expression of LC3 and N protein under these two pharmacological conditions by performing confocal microscopy. Similarly, MK2206 triggered the formation of LC3 puncta and promoted viral replication while Neferine displayed an opposite effect (Figure 5G). Viral titration was used to assess the viral production in pharmacological experiments. Using untreated infected cells as control, treatment of MK2206 increased the viral load in the supernatant while Neferine decreased it (Figure 5H). Finally, we conducted the RNA interference experiment and designed three siRNAs targeting Akt, of which only siAkt-1 showed significant inhibition (Figure 5I). Thus, siAkt-1 was selected for the subsequent virus infection experiment. Vero E6 cells were infected with SADS-CoV after the transfection of siNC or siAkt-1 for 24 h, and the cell lysates were collected at 24 hpi for western blotting and viral titration, respectively. Knockdown of Akt resulted in reduced level of p-Akt and p-mTOR, and the expression of LC3-II and viral N protein were both enhanced (Figures 5J and 5K). Similar observations were obtained by viral titer assay (Figure 5L). Collectively, SADS-CoV appears to induce autophagy via the suppression of the Akt/mTOR pathway, and thus facilitates its proliferation.

Integrin α3 prevents Swine acute diarrhea syndrome coronavirus production through autophagy inhibition

To further gain insight into the mechanism of SADS-CoV-induced autophagy, proteome research of SADS-CoV infected Vero E6 cells was performed at 24 hpi (Figure S2 and Table S1). Kyoto Encyclopedia of Genes and Genomes (KEGG) pathway analysis revealed that multiple cellular pathways corresponding to the SADS-CoV infection were highly enriched, including the PI3K/Akt pathway, which was thought to be one of the most important signal cascades upstream of mTOR (Figure 6A). The differentially altered proteins in PI3K/Akt pathway were picked out for cluster analysis (Figure 6A). Based on the above studies of Akt/mTOR and relevant literature, we selected eight PI3K/Akt-related candidate proteins for preliminary screening of their effects on viral proliferation. Western blotting indicated that integrin α3 (ITGA3) suppressed the expression level of viral N protein (Figures 6D and 6E), whereas others had no obvious antiviral properties (data not shown). Besides, endogenous expression change of ITGA3 in response to SADS-CoV infection was confirmed at 24 and 36 hpi, which was consistent with its downregulation in proteome profiles (Figures 6A-6C). Virus titer assay showed a similar observation that overexpression of ITGA3 noticeably decreased viral yield (Figure 6F). Hence, we further explored the antiviral mechanism of ITGA3.

ITGA3 belongs to a large family of transmembrane glycoproteins that are essential for the cell matrix attachment and act as signal transducers for various cellular biological processes (Ramovs et al., 2021; Vlahakis and Debnath, 2017). Furthermore, it has been found that integrin is also closely related to autophagy (Vlahakis and Debnath, 2017). We consequently speculated that ITGA3 might inhibit virus replication through autophagy. To verify our suppose, the level of LC3 conversion in cells overexpressing ITGA3 was assessed during SADS-CoV infection, and LC3-II expression was indeed downregulated compared to empty vector-transfected cells (Figure 6D). Due to the above-mentioned role of the Akt/mTOR pathway in the SADS-CoV-induced autophagy, we evaluated the phosphorylation of Akt and mTOR in infected cells transfected with ITGA3 overexpression vector or empty vector. Exogenous expression of ITGA3 did not lead to significant changes in the total protein level of Akt and mTOR, but resulted in the upregulation of their phosphorylation, suggesting activation of Akt/mTOR signal cascade (Figure 6G). These findings implied that Akt/mTOR pathway might be an intermediate signal bridge between ITGA3 and autophagy. In addition, RNA interference was employed for further validation. We designed three siRNAs targeting ITGA3, among which siITGA3-3 showed the best inhibitory effect (Figure 6H). Vero E6 cells were infected with SADS-CoV after the transfection of siNC or siITGA3 for 24 h, and the cell deposits and supernatant were harvested at 24 hpi for western blotting and viral titration, respectively. In line with expectation, the LC3-II and viral N protein expression were both enhanced in the ITGA3-knockdown cells compared with the level in the NC-knockdown cells during viral infection (Figures 6I and 6J). Similar observations were obtained through viral titer assay (Figure 6K). Likewise, we examined Akt and mTOR activation status

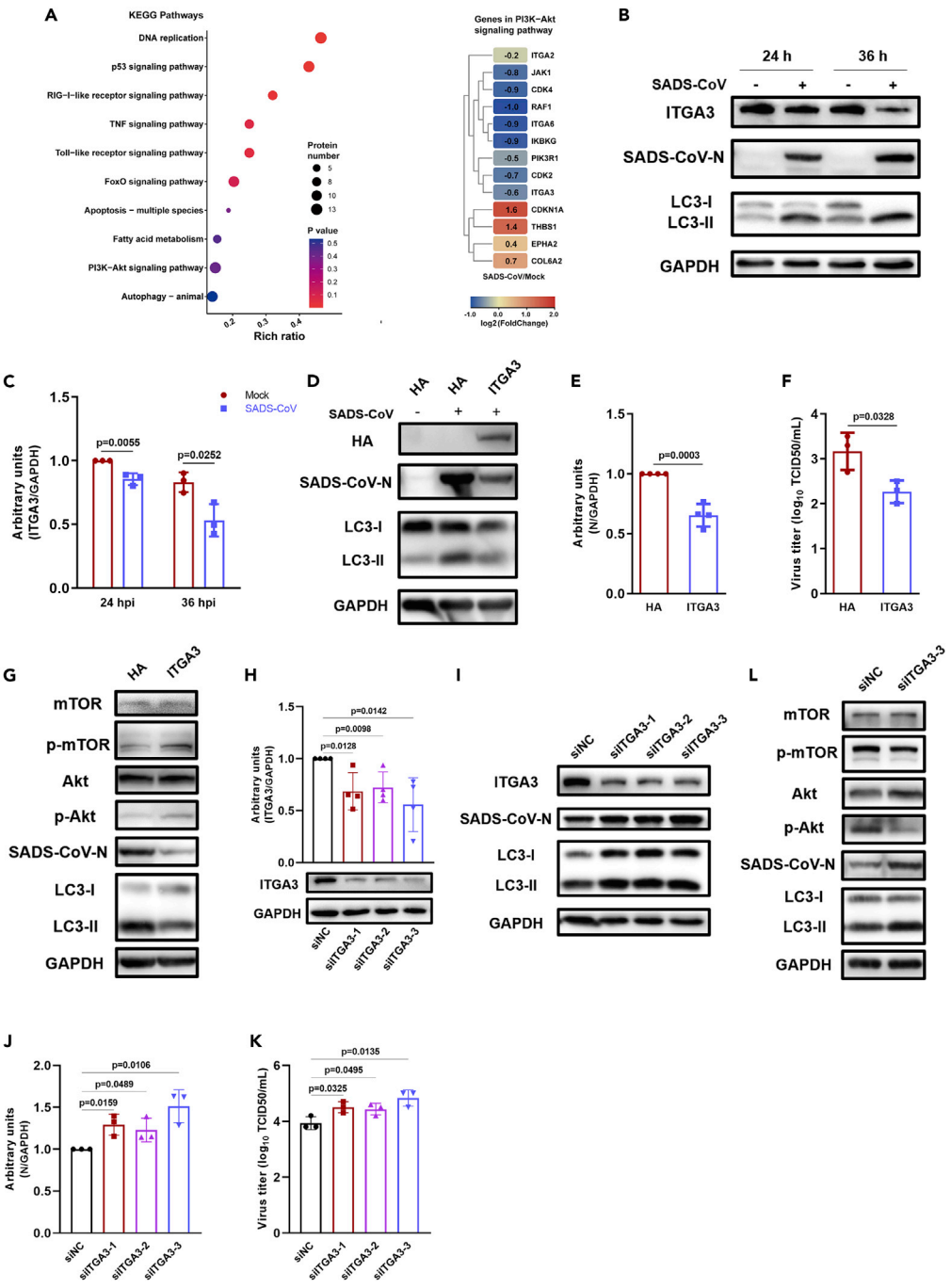

Figure 6. ITGA3 suppresses SADS-CoV replication through autophagy inhibition

(A) Dot map (left) shows the compilation of the top 14 enriched Kyoto encyclopedia of genes and genomes (KEGG) pathways in all SADS-CoV infection groups. Each vertical column of the dot represents a SADS-CoV infection group. Heatmap (right) shows the fold change of genes in four KEGG pathways in SADS-CoV-infected cells compared with mock-infected cells at 24 hpi.

(B) Vero E6 cells were mock infected or infected with SADS-CoV (MOI = 0.1) and were collected at 24 and 36 hpi. Cell samples were then processed for Western blot analysis.

(C) The normalized ratios of ITGA3 to GAPDH at different time points.

(D) Vero E6 cells were transfected with pcDNA3.1(+)-HA or pcDNA3.1(+)-HA-ITGA3 and were infected with SADS-CoV (MOI = 0.1) after 24 h transfection. Cell lysates were collected and subjected to Western blot analysis at 24 hpi.

(E) The SADS-CoV-N levels relative to the GAPDH levels were determined by densitometry.

Figure 6. *Continued*

(F) The viral titer of the culture supernatant was measured by $TCID_{50}$.

(G) Vero E6 cells were prepared as described in the legend of Figure 6D. The effect of the overexpressed exogenous ITGA3 on the level of Akt and mTOR activities and the replication of SADS-CoV were measured with indicated antibodies.

(H) Vero E6 cells were transfected with siITGA3 or siNC and were harvested for Western blot analysis at 48 hpi. Knockdown efficiency of specific siRNA was tested by the relative expression of ITGA3 to GAPDH.

(I) Vero E6 cells treated with the indicated siRNAs were infected with SADS-CoV (MOI = 0.1) after 24 h transfection. Then the cells were harvested at 24 hpi and subjected to Western blot analysis.

(J) The normalized ratios of SADS-CoV-N/GAPDH in different transfected cells.

(K) The viral titer of the culture supernatant was determined by $TCID_{50}$.

(L) Vero E6 cells were prepared as described in the legend of Figure 6I. The effect of the knockdown of ITGA3 on the level of Akt and mTOR activities and the viral replication was measured with indicated antibodies. The data presented are means ± SD from at least three independent experiments.

in siITGA3-3 transfected cells and the results displayed a lower phosphorylation level of Akt and mTOR, indicating stronger inhibition of the Akt/mTOR pathway (Figure 6L). Together, these findings suggest that SADS-CoV could induce autophagy through the regulation of ITGA3, which might be mediated by the Akt/mTOR pathway.

DISCUSSION

In mammalian cells, macromolecular homeostasis requires selective degradation of damaged units, which is mainly mediated by two proteolytic systems: the ubiquitin-proteasome system (UPS) and the autophagy-lysosome system (Chen et al., 2021). UPS is the major extra-lysosomal pathway for protein degradation, in which proteins, especially short-lived proteins, are selectively labeled with ubiquitin tags for destruction (Rousseau and Bertolotti, 2018). In contrast, autophagy degrades proteins via engulfing cytoplasmic cargo through autophagosomes, including long-lived proteins, protein aggregates, organelles, RNA, and DNA, and delivers this cargo to lysosomes for degradation (Levine and Kroemer, 2019). Therefore, the host often uses the degradation function of autophagy as one of the powerful tools to defend against viral infection. For the coronavirus family, many viruses have been shown to induce autophagy, while SADS-CoV remains unclear. Here, we clearly show that SADS-CoV infection promotes the conversion of LC3-I to LC3-II, and increases the formation of punctate LC3 proteins and cytoplasmic DMVs in Vero cells and IPI-FX cells, demonstrating that SADS-CoV infection can trigger the cellular autophagy pathway. Notably, coronavirus-induced DMVs, structurally similar to autophagosomes, are thought to provide a platform for viral RNA synthesis. Evidence that autophagy proteins are involved in the formation of DMVs in rhinovirus and poliovirus-infected cells indicates that DMVs may come from the viral hijacking of the host autophagy pathway (Jackson et al., 2005).

Previous studies have revealed that the interaction between coronavirus and autophagy is very complex and diverse, which is difficult to generalized. As a protective catabolic process, activation of autophagy reduces MERS-CoV replication, and the deletion of ATG 5 rescues the survival of the virus in Vero B4 cells (Gassen et al., 2019). However, some porcine CoVs, such as PEDV and transmissible gastroenteritis virus (TGEV), select a strategy to facilitate their proliferation by inducing autophagy (Guo et al., 2017; Zhu et al., 2016). In addition, the classical autophagy pathway may not be necessary for avian infectious bronchitis virus (IBV) replication, for the induction or inhibition of autophagy does not affect its replication (Maier et al., 2013), but it does not rule out whether a single autophagic component has an effect. To further investigate the role of autophagy in viral infection, we treated cells with autophagy regulators. Our results showed that viral replication increased after treatment with autophagy inducer rapamycin; in contrast, the autophagy inhibitor 3MA reduced it, suggesting a proviral role of autophagy in SADS-CoV infection. Nevertheless, some coronavirus can induce autophagy but block the fusion process of autophagosome and lysosome in the later stage to escape degradation (Chen et al., 2014). It was reported that ORF3a of the SARS-CoV-2 inhibited autophagy activity by blocking the fusion of autophagosomes/amphisomes with lysosomes (Miao et al., 2021). Thus, we used Baf A1, an inhibitor that can block the autophagosome-lysosome fusion, to investigate whether SADS-CoV replication needed autophagy flux. The observation of the accumulation of LC3-II, but the reduction of SADS-CoV-N protein indicated that viral proliferation required the complete autophagy pathway. Actually, similar results have previously been found in some other coronaviruses. Human coronavirus HCoV-OC43 infection increased autophagic flux in MRC-5 cells, while treatment with kurarinone to impair the flux inhibited viral replication (Min et al., 2020). The autophagy flux also elevated in PEDV-infected Vero cell, but could be suppressed by

chloroquine (CQ), an inhibitor of autophagosome-lysosome fusion, and as a consequence, the yield of PEDV was decreased (Guo et al., 2017). We speculated that the virus utilized the membrane structure of autolysosomes in a way similar to DMVs to facilitate its proliferation, and as a supporting example, Ke et al. found that HCV-activated autolysosome formation was essential for viral RNA replication (Ke and Chen, 2011b). Clearly, further mechanistic research to elucidate the interaction between SADS-CoV and autophagy is warranted.

The mTOR pathway plays a pivotal role in autophagy activation; and meanwhile, is an important integrator of metabolic, growth factor, and energy signals in orchestrating cell metabolism and innate immune responses under the regulation of the Akt kinase (Diaz-Troya et al., 2008; Yang et al., 2020). Previous work of transcriptome in Vero E6 cells (Zeng et al., 2021) suggested significant changes in Akt/mTOR signaling cascade during SADS-CoV infection. Therefore, to define the upstream signal that led to SADS-CoV-induced autophagy, we analyzed the Akt/mTOR pathway. Our research showed that the total protein levels of Akt and mTOR did not change significantly with the course of infection, but both phosphorylations were downregulation. Pharmacological treatment using Akt regulator Neferine inhibited autophagy and subsequently, the viral proliferation was decreased. On the contrary, suppression of Akt signaling by MK2206 led to the induction of autophagy and an increase in viral yield. These findings revealed that SADS-CoV could modulate the Akt/mTOR pathway to usurp autophagy as a survival strategy. Actually, many other viruses also target this pathway in a similar way to evade host supervision and facilitate their own replication. For instance, alphaherpesvirus US3 could inhibit autophagy levels via activation of the Akt/mTOR pathway, thereby escaping host clearance (Sun et al., 2017). Since the critical role of this pathway in regulating various cell functions, it is often a powerful target for anti-coronavirus pharmaceutical intervention. Maria et al. summarized the potential therapeutic and prophylactic effects of targeting the PI3K/Akt/mTOR axis on SARS-CoV-2 infection (Basile et al., 2022), which provided valuable pharmacological strategies for the management of COVID-19 treatment. Of note, Akt inhibitor MK-2206 significantly reduced the yield of SARS-CoV-2 *in vitro* (Appelberg et al., 2020). The opposite pharmacological effects on SARS-CoV-2 and SADS-CoV are most likely due to diverse regulatory functions of autophagy during the life cycle of different coronaviruses (Gassen et al., 2021). Another inhibitor GSK690693 could induce autophagy through Akt/mTOR signaling pathway, and thereby enhancing PEDV replication, which is also a swine diarrhea coronavirus similar to SADS-CoV (Lin et al., 2020). In a word, future research on the therapeutic effects of specific inhibitors of PI3K/Akt/mTOR pathway could be extended to more coronavirus.

Given that Akt is a kinase, further insight into the mechanism of SADS-CoV-induced autophagy may be provided by investigating the upstream events of the Akt/mTOR pathway. In order to excavate possible functional proteins, we performed proteomics to screen the differentially changed pathways and related proteins during SADS-CoV infection in Vero E6 cells. Of the significantly altered genes in the Akt-related pathway, we identified ITGA3, a member of the integrin family, as a potential antiviral regulator. Interestingly, transmembrane glycoproteins integrins not only mediate cell-matrix adhesion but also regulate a variety of intracellular kinase activation pathways (Izmailyan et al., 2012; Ramovs et al., 2021). Integrin β1 has been reported to mediate vaccinia virus entry in both mouse embryonic fibroblast and HeLa cells in a manner of PI3K/Akt signaling activation (Izmailyan et al., 2012). In breast cancer, the downregulation of ITGA3 inhibited the activity of the PI3K-Akt axis and promoted cell proliferation, apoptosis, invasion, and migration (Zhang et al., 2020). In addition, it seems that some β-integrin proteins are likely to act in the cell entry system of SARS-CoV-2 through their short linear motif and LC3-interacting region motif (Meszaros et al., 2021), implying a potential link between SARS-CoV-2, integrin, and autophagy. Actually, several previous researches indicated an inverse relationship between autophagy and integrin. Integrin β3 inhibited lipopolysaccharide-induced autophagy in cardiomyocytes (Zhu et al., 2015). Likewise, blockage of integrin α3β1 function is sufficient to activate autophagy in mammary epithelial cells (Chen and Debnath, 2013). Here, we also found that exogenous expression of ITGA3 inhibited SADS-CoV proliferation through the suppression of autophagy, and this effect could be medicated by Akt/mTOR signal cascade. The observation revealed a strong link between integrin, autophagy, and viral survival; however, more studies will be needed to dissect the interaction between SADS-CoV and integrins in the future.

Collectively, our study shows that SADS-CoV infection induces the autophagy pathway to facilitate its replication in Vero E6 cells and IPI-FX cells, while pharmacological inhibition of autophagy reduces viral yield. Importantly, based on transcriptomic and proteomic research, we infer and validate an axis of ITGA3-mediated autophagy upon SADS-CoV infection. Akt/mTOR pathway activation is negatively correlated with

autophagy induction, and ITGA3 is one of the functional regulators upstream of Akt kinase. These findings could contribute to the understanding of the host antiviral response and the development of novel antiviral therapies to prevent and control SADS-CoV infection.

Limitations of the study

In this study, we demonstrated that ITGA3 prevented SADS-CoV production through autophagy inhibition in Vero E6 cells. In many coronavirus-related researches, Vero E6 cells are often used as a model system due to the highly permissible virus infection, including SADS-CoV. However, pigs are the natural host of SADS-CoV, while the Vero E6 cell is a kidney cell line from the African green monkey. Since there could be some variation in signal transduction pathways among different cell types, future studies to dissect the role of the Akt/mTOR pathway and ITGA3 in pig cells infected with SADS-CoV will be important extensions of this work.

STAR★METHODS

Detailed methods are provided in the online version of this paper and include the following:

- KEY RESOURCES TABLE
- RESOURCE AVAILABILITY
  - Lead contact
  - Materials availability
  - Data and code availability
- EXPERIMENTAL MODEL AND SUBJECT DETAILS
  - Cells and viruses
- METHOD DETAILS
  - Viral infection and drug treatment
  - Plasmids and siRNAs
  - Western blotting
  - Confocal immunofluorescence microscopy
  - Transmission electron microscopy
  - Cell viability assay
  - Proteomic assay
- QUANTIFICATION AND STATISTICAL ANALYSIS

SUPPLEMENTAL INFORMATION

Supplemental information can be found online at https://doi.org/10.1016/j.isci.2022.105394.

ACKNOWLEDGMENTS

This work was supported by the National Key Research and Development Program of China (No. 2021YFD1801102 and 2018YFD0501102) and Guangdong Natural Science Foundation (No. 2018B030314003). We thank Professor Shaobo Xiao (Huazhong Agricultural University, Wuhan, China) for kindly providing us with porcine ileum epithelial cell line (IPI-FX).

AUTHOR CONTRIBUTIONS

Conceptualization, H.Z. and S.Z.; methodology, S.Z.; experiments, S.Z., Y.Z., Y.X., and H.L.; software, O.*P. and* H.Z.; writing—original draft preparation, S.Z., Y.Z., and O.P.; writing—review and editing, H.Z., Q.X.; supervision, H.Z., Y.C., and C.X.; project administration, H.Z.; funding acquisition, H.Z., Y.C., and C.X. All authors have read and agreed to the published version of the article.

DECLARATION OF INTERESTS

The authors declare no competing interests.

Received: January 4, 2022
Revised: August 6, 2022
Accepted: October 14, 2022
Published: November 18, 2022

REFERENCES

Angelini, M.M., Akhlaghpour, M., Neuman, B.W., and Buchmeier, M.J. (2013). Severe acute respiratory syndrome coronavirus nonstructural proteins 3, 4, and 6 induce double-membrane vesicles. mBio *4*. https://doi.org/10.1128/mBio.00524-13.

Appelberg, S., Gupta, S., Svensson Akusjärvi, S., Ambikan, A.T., Mikaeloff, F., Saccon, E., Végvári, Á., Benfeitas, R., Sperk, M., Ståhlberg, M., et al. (2020). Dysregulation in Akt/mTOR/HIF-1 signaling identified by proteo-transcriptomics of SARS-CoV-2 infected cells. Emerg. Microb. Infect. *9*, 1748–1760. https://doi.org/10.1080/22221751.2020.1799723.

Barth, S., Glick, D., and Macleod, K.F. (2010). Autophagy: assays and artifacts. J. Pathol. *221*, 117–124. https://doi.org/10.1002/path.2694.

Basile, M.S., Cavalli, E., McCubrey, J., Hernández-Bello, J., Muñoz-Valle, J.F., Fagone, P., and Nicoletti, F. (2022). The PI3K/Akt/mTOR pathway: a potential pharmacological target in COVID-19. Drug Discov. Today *27*, 848–856. https://doi.org/10.1016/j.drudis.2021.11.002.

Baskaran, R., Poornima, P., Priya, L.B., Huang, C.Y., and Padma, V.V. (2016). Neferine prevents autophagy induced by hypoxia through activation of Akt/mTOR pathway and Nrf2 in muscle cells. Biomed. Pharmacother. *83*, 1407–1413. https://doi.org/10.1016/j.biopha.2016.08.063.

Boya, P., Reggiori, F., and Codogno, P. (2013). Emerging regulation and functions of autophagy. Nat. Cell Biol. *15*, 713–720. https://doi.org/10.1038/ncb2788.

Chang, H., Li, X., Cai, Q., Li, C., Tian, L., Chen, J., Xing, X., Gan, Y., Ouyang, W., and Yang, Z. (2017). The PI3K/Akt/mTOR pathway is involved in CVB3-induced autophagy of HeLa cells. Int. J. Mol. Med. *40*, 182–192. https://doi.org/10.3892/ijmm.2017.3008.

Chen, N., and Debnath, J. (2013). IkappaB kinase complex (IKK) triggers detachment-induced autophagy in mammary epithelial cells independently of the PI3K-AKT-MTORC1 pathway. Autophagy *9*, 1214–1227. https://doi.org/10.4161/auto.24870.

Chen, X., Wang, K., Xing, Y., Tu, J., Yang, X., Zhao, Q., Li, K., and Chen, Z. (2014). Coronavirus membrane-associated papain-like proteases induce autophagy through interacting with Beclin1 to negatively regulate antiviral innate immunity. Protein Cell *5*, 912–927. https://doi.org/10.1007/s13238-014-0104-6.

Chen, X., Yu, C., Kang, R., Kroemer, G., and Tang, D. (2021). Cellular degradation systems in ferroptosis. Cell Death Differ. *28*, 1135–1148. https://doi.org/10.1038/s41418-020-00728-1.

Chin, C.H., Chen, S.H., Wu, H.H., Ho, C.W., Ko, M.T., and Lin, C.Y. (2014). cytoHubba: identifying hub objects and sub-networks from complex interactome. BMC Syst. Biol. *8*, S11. https://doi.org/10.1186/1752-0509-8-S4-S11.

Corman, V.M., Eckerle, I., Bleicker, T., Zaki, A., Landt, O., Eschbach-Bludau, M., van Boheemen, S., Gopal, R., Ballhause, M., Bestebroer, T.M., et al. (2012). Detection of a novel human coronavirus by real-time reverse-transcription polymerase chain reaction. Euro Surveill. *17*, 20285. https://doi.org/10.2807/ese.17.39.20285-en.

Díaz-Troya, S., Pérez-Pérez, M.E., Florencio, F.J., and Crespo, J.L. (2008). The role of TOR in autophagy regulation from yeast to plants and mammals. Autophagy *4*, 851–865. https://doi.org/10.4161/auto.6555.

Dong, X., and Levine, B. (2013). Autophagy and viruses: adversaries or allies? J. Innate Immun. *5*, 480–493. https://doi.org/10.1159/000346388.

Dreux, M., and Chisari, F.V. (2010). Viruses and the autophagy machinery. Cell Cycle *9*, 1295–1307. https://doi.org/10.4161/cc.9.7.11109.

Drosten, C., Günther, S., Preiser, W., van der Werf, S., Brodt, H.R., Becker, S., Rabenau, H., Panning, M., Kolesnikova, L., Fouchier, R.A.M., et al. (2003). Identification of a novel coronavirus in patients with severe acute respiratory syndrome. N. Engl. J. Med. *348*, 1967–1976. https://doi.org/10.1056/NEJMoa030747.

Edwards, C.E., Yount, B.L., Graham, R.L., Leist, S.R., Hou, Y.J., Dinnon, K.H., 3rd, Sims, A.C., Swanstrom, J., Gully, K., Scobey, T.D., et al. (2020). Swine acute diarrhea syndrome coronavirus replication in primary human cells reveals potential susceptibility to infection. Proc. Natl. Acad. Sci. USA *117*, 26915–26925. https://doi.org/10.1073/pnas.2001046117.

Gassen, N.C., Niemeyer, D., Muth, D., Corman, V.M., Martinelli, S., Gassen, A., Hafner, K., Papies, J., Mösbauer, K., Zellner, A., et al. (2019). SKP2 attenuates autophagy through Beclin1-ubiquitination and its inhibition reduces MERS-Coronavirus infection. Nat. Commun. *10*, 5770. https://doi.org/10.1038/s41467-019-13659-4.

Gassen, N.C., Papies, J., Bajaj, T., Emanuel, J., Dethloff, F., Chua, R.L., Trimpert, J., Heinemann, N., Niemeyer, C., Weege, F., et al. (2021). SARS-CoV-2-mediated dysregulation of metabolism and autophagy uncovers host-targeting antivirals. Nat. Commun. *12*, 3818. https://doi.org/10.1038/s41467-021-24007-w.

Gong, L., Li, J., Zhou, Q., Xu, Z., Chen, L., Zhang, Y., Xue, C., Wen, Z., and Cao, Y. (2017). A new bat-HKU2-like coronavirus in swine, China, 2017. Emerg. Infect. Dis. *23*, 1607–1609. https://doi.org/10.3201/eid2309.170915.

Guo, X., Zhang, M., Zhang, X., Tan, X., Guo, H., Zeng, W., Yan, G., Memon, A.M., Li, Z., Zhu, Y., et al. (2017). Porcine epidemic diarrhea virus induces autophagy to benefit its replication. Viruses *9*, E53. https://doi.org/10.3390/v9030053.

Hait, A.S., Olagnier, D., Sancho-Shimizu, V., Skipper, K.A., Helleberg, M., Larsen, S.M., Bodda, C., Moldovan, L.I., Ren, F., Brinck Andersen, N.S., et al. (2020). Defects in LC3B2 and ATG4A underlie HSV2 meningitis and reveal a critical role for autophagy in antiviral defense in humans. Sci. Immunol. *5*, eabc2691. https://doi.org/10.1126/sciimmunol.abc2691.

He, C., and Klionsky, D.J. (2009). Regulation mechanisms and signaling pathways of autophagy. Annu. Rev. Genet. *43*, 67–93. https://doi.org/10.1146/annurev-genet-102808-114910.

Herrewegh, A.A., Smeenk, I., Horzinek, M.C., Rottier, P.J., and de Groot, R.J. (1998). Feline coronavirus type II strains 79-1683 and 79-1146 originate from a double recombination between feline coronavirus type I and canine coronavirus. J. Virol. *72*, 4508–4514. https://doi.org/10.1128/JVI.72.5.4508-4514.1998.

Hui, X., Zhang, L., Cao, L., Huang, K., Zhao, Y., Zhang, Y., Chen, X., Lin, X., Chen, M., and Jin, M. (2021). SARS-CoV-2 promote autophagy to suppress type I interferon response. Signal Transduct. Targeted Ther. *6*, 180. https://doi.org/10.1038/s41392-021-00574-8.

Izmailyan, R., Hsao, J.C., Chung, C.S., Chen, C.H., Hsu, P.W.C., Liao, C.L., and Chang, W. (2012). Integrin beta1 mediates vaccinia virus entry through activation of PI3K/Akt signaling. J. Virol. *86*, 6677–6687. https://doi.org/10.1128/JVI.06860-11.

Jackson, W.T., Giddings, T.H., Jr., Taylor, M.P., Mulinyawe, S., Rabinovitch, M., Kopito, R.R., and Kirkegaard, K. (2005). Subversion of cellular autophagosomal machinery by RNA viruses. PLoS Biol. *3*, e156. https://doi.org/10.1371/journal.pbio.0030156.

Jia, X., Chen, Y., Zhao, X., Lv, C., and Yan, J. (2016). Oncolytic vaccinia virus inhibits human hepatocellular carcinoma MHCC97-H cell proliferation via endoplasmic reticulum stress, autophagy and Wnt pathways. J. Gene Med. *18*, 211–219. https://doi.org/10.1002/jgm.2893.

Kanehisa, M., Furumichi, M., Sato, Y., Ishiguro-Watanabe, M., and Tanabe, M. (2021). KEGG: integrating viruses and cellular organisms. Nucleic Acids Res. *49*, D545–D551. https://doi.org/10.1093/nar/gkaa970.

Ke, P.Y., and Chen, S.S.L. (2011a). Autophagy: a novel guardian of HCV against innate immune response. Autophagy *7*, 533–535. https://doi.org/10.4161/auto.7.5.14732.

Ke, P.Y., and Chen, S.S.L. (2011b). Activation of the unfolded protein response and autophagy after hepatitis C virus infection suppresses innate antiviral immunity in vitro. J. Clin. Invest. *121*, 37–56. https://doi.org/10.1172/JCI41474.

King, J.S., Veltman, D.M., and Insall, R.H. (2011). The induction of autophagy by mechanical stress. Autophagy *7*, 1490–1499. https://doi.org/10.4161/auto.7.12.17924.

Kroemer, G., Mariño, G., and Levine, B. (2010). Autophagy and the integrated stress response. Mol. Cell *40*, 280–293. https://doi.org/10.1016/j.molcel.2010.09.023.

Lednicky, J.A., Tagliamonte, M.S., White, S.K., Elbadry, M.A., Alam, M.M., Stephenson, C.J., Bonny, T.S., Loeb, J.C., Telisma, T., Chavannes, S., et al. (2021). Independent infections of porcine deltacoronavirus among Haitian children. Nature *600*, 133–137. https://doi.org/10.1038/s41586-021-04111-z.

Levine, B., and Kroemer, G. (2019). Biological functions of autophagy genes: a disease perspective. Cell *176*, 11–42. https://doi.org/10.1016/j.cell.2018.09.048.

Liang, Q., Luo, Z., Zeng, J., Chen, W., Foo, S.S., Lee, S.A., Ge, J., Wang, S., Goldman, S.A., Zlokovic, B.V., et al. (2016). Zika virus NS4A and NS4B proteins deregulate akt-mTOR signaling in human fetal neural stem cells to inhibit neurogenesis and induce autophagy. Cell Stem Cell *19*, 663–671. https://doi.org/10.1016/j.stem.2016.07.019.

Lin, H., Li, B., Liu, M., Zhou, H., He, K., and Fan, H. (2020). Nonstructural protein 6 of porcine epidemic diarrhea virus induces autophagy to promote viral replication via the PI3K/Akt/mTOR axis. Vet. Microbiol. *244*, 108684. https://doi.org/10.1016/j.vetmic.2020.108684.

Luo, Y., Chen, Y., Geng, R., Li, B., Chen, J., Zhao, K., Zheng, X.S., Zhang, W., Zhou, P., Yang, X.L., and Shi, Z.L. (2021). Broad cell tropism of SADS-CoV in vitro implies its potential cross-species infection risk. Virol. Sin. *36*, 559–563. https://doi.org/10.1007/s12250-020-00321-3.

Ma, J., Sun, Q., Mi, R., and Zhang, H. (2011). Avian influenza A virus H5N1 causes autophagy-mediated cell death through suppression of mTOR signaling. J GENET GENOMICS *38*, 533–537. https://doi.org/10.1016/j.jgg.2011.10.002.

Maier, H.J., Cottam, E.M., Stevenson-Leggett, P., Wilkinson, J.A., Harte, C.J., Wileman, T., and Britton, P. (2013). Visualizing the autophagy pathway in avian cells and its application to studying infectious bronchitis virus. Autophagy *9*, 496–509. https://doi.org/10.4161/auto.23465.

Manning, B.D., and Toker, A. (2017). AKT/PKB signaling: navigating the network. Cell *169*, 381–405. https://doi.org/10.1016/j.cell.2017.04.001.

Mattoscio, D., Medda, A., and Chiocca, S. (2018). Human papilloma virus and autophagy. Int. J. Mol. Sci. *19*, E1775. https://doi.org/10.3390/ijms19061775.

Mészáros, B., Sámano-Sánchez, H., Alvarado-Valverde, J., Čalyševa, J., Martínez-Pérez, E., Alves, R., Shields, D.C., Kumar, M., Rippmann, F., Chemes, L.B., and Gibson, T.J. (2021). Short linear motif candidates in the cell entry system used by SARS-CoV-2 and their potential therapeutic implications. Sci. Signal. *14*, eabd0334. https://doi.org/10.1126/scisignal.abd0334.

Miao, G., Zhao, H., Li, Y., Ji, M., Chen, Y., Shi, Y., Bi, Y., Wang, P., and Zhang, H. (2021). ORF3a of the COVID-19 virus SARS-CoV-2 blocks HOPS complex-mediated assembly of the SNARE complex required for autolysosome formation. Dev. Cell *56*, 427–442.e5. https://doi.org/10.1016/j.devcel.2020.12.010.

Millet, J.K., Jaimes, J.A., and Whittaker, G.R. (2021). Molecular diversity of coronavirus host cell entry receptors. FEMS Microbiol. Rev. *45*, fuaa057. https://doi.org/10.1093/femsre/fuaa057.

Min, J.S., Kim, D.E., Jin, Y.H., and Kwon, S. (2020). Kurarinone inhibits HCoV-OC43 infection by impairing the virus-induced autophagic flux in MRC-5 human lung cells. J. Clin. Med. *9*, E2230. https://doi.org/10.3390/jcm9072230.

Mizushima, N. (2009). Physiological functions of autophagy. Curr. Top. Microbiol. Immunol. *335*, 71–84. https://doi.org/10.1007/978-3-642-00302-8_3.

Mizushima, N., Yamamoto, A., Hatano, M., Kobayashi, Y., Kabeya, Y., Suzuki, K., Tokuhisa, T., Ohsumi, Y., and Yoshimori, T. (2001). Dissection of autophagosome formation using Apg5-deficient mouse embryonic stem cells. J. Cell Biol. *152*, 657–668. https://doi.org/10.1083/jcb.152.4.657.

Mizushima, N., Yoshimori, T., and Levine, B. (2010). Methods in mammalian autophagy research. Cell *140*, 313–326. https://doi.org/10.1016/j.cell.2010.01.028.

Mohamud, Y., Shi, J., Qu, J., Poon, T., Xue, Y.C., Deng, H., Zhang, J., and Luo, H. (2018). Enteroviral infection inhibits autophagic flux via disruption of the SNARE complex to enhance viral replication. Cell Rep. *22*, 3292–3303. https://doi.org/10.1016/j.celrep.2018.02.090.

Oudshoorn, D., Rijs, K., Limpens, R.W.A.L., Groen, K., Koster, A.J., Snijder, E.J., Kikkert, M., and Bárcena, M. (2017). Expression and cleavage of Middle East respiratory syndrome coronavirus nsp3-4 polyprotein induce the formation of double-membrane vesicles that mimic those associated with coronaviral RNA replication. mBio *8*. https://doi.org/10.1128/mBio.01658-17.

Pan, Y., Tian, X., Qin, P., Wang, B., Zhao, P., Yang, Y.L., Wang, L., Wang, D., Song, Y., Zhang, X., and Huang, Y.W. (2017). Discovery of a novel swine enteric alphacoronavirus (SeACoV) in southern China. Vet. Microbiol. *211*, 15–21. https://doi.org/10.1016/j.vetmic.2017.09.020.

Ramovs, V., Krotenberg Garcia, A., Kreft, M., and Sonnenberg, A. (2021). Integrin alpha3beta1 is a key regulator of several protumorigenic pathways during skin carcinogenesis. J. Invest. Dermatol. *141*, 732–741.e6. https://doi.org/10.1016/j.jid.2020.07.024.

Reggiori, F., Monastyrska, I., Verheije, M.H., Calì, T., Ulasli, M., Bianchi, S., Bernasconi, R., de Haan, C.A.M., and Molinari, M. (2010). Coronaviruses Hijack the LC3-I-positive EDEMosomes, ER-derived vesicles exporting short-lived ERAD regulators, for replication. Cell Host Microbe *7*, 500–508. https://doi.org/10.1016/j.chom.2010.05.013.

Richards, A.L., and Jackson, W.T. (2013). How positive-strand RNA viruses benefit from autophagosome maturation. J. Virol. *87*, 9966–9972. https://doi.org/10.1128/JVI.00460-13.

Rousseau, A., and Bertolotti, A. (2018). Regulation of proteasome assembly and activity in health and disease. Nat. Rev. Mol. Cell Biol. *19*, 697–712. https://doi.org/10.1038/s41580-018-0040-z.

Sahoo, B.R., Pattnaik, A., Annamalai, A.S., Franco, R., and Pattnaik, A.K. (2020). Mechanistic target of rapamycin signaling activation antagonizes autophagy to facilitate Zika virus replication. J. Virol. *94*. https://doi.org/10.1128/JVI.01575-20.

Shannon, P., Markiel, A., Ozier, O., Baliga, N.S., Wang, J.T., Ramage, D., Amin, N., Schwikowski, B., and Ideker, T. (2003). Cytoscape: a software environment for integrated models of biomolecular interaction networks. Genome Res. *13*, 2498–2504. https://doi.org/10.1101/gr.1239303.

Snijder, E.J., Limpens, R.W.A.L., de Wilde, A.H., de Jong, A.W.M., Zevenhoven-Dobbe, J.C., Maier, H.J., Faas, F.F.G.A., Koster, A.J., and Bárcena, M. (2020). A unifying structural and functional model of the coronavirus replication organelle: tracking down RNA synthesis. PLoS Biol. *18*, e3000715. https://doi.org/10.1371/journal.pbio.3000715.

Sumpter, R., Jr., and Levine, B. (2011). Selective autophagy and viruses. Autophagy *7*, 260–265. https://doi.org/10.4161/auto.7.3.14281.

Sun, M., Hou, L., Tang, Y.D., Liu, Y., Wang, S., Wang, J., Shen, N., An, T., Tian, Z., and Cai, X. (2017). Pseudorabies virus infection inhibits autophagy in permissive cells in vitro. Sci. Rep. *7*, 39964. https://doi.org/10.1038/srep39964.

Sun, P., Zhang, S., Qin, X., Chang, X., Cui, X., Li, H., Zhang, S., Gao, H., Wang, P., Zhang, Z., et al. (2018). Foot-and-mouth disease virus capsid protein VP2 activates the cellular EIF2S1-ATF4 pathway and induces autophagy via HSPB1. Autophagy *14*, 336–346. https://doi.org/10.1080/15548627.2017.1405187.

Szklarczyk, D., Gable, A.L., Nastou, K.C., Lyon, D., Kirsch, R., Pyysalo, S., Doncheva, N.T., Legeay, M., Fang, T., Bork, P., et al. (2021). The STRING database in 2021: customizable protein-protein networks, and functional characterization of user-uploaded gene/measurement sets. Nucleic Acids Res. *49*, D605–D612. https://doi.org/10.1093/nar/gkaa1074.

van der Meer, Y., Snijder, E.J., Dobbe, J.C., Schleich, S., Denison, M.R., Spaan, W.J., and Locker, J.K. (1999). Localization of mouse hepatitis virus nonstructural proteins and RNA synthesis indicates a role for late endosomes in viral replication. J. Virol. *73*, 7641–7657. https://doi.org/10.1128/JVI.73.9.7641-7657.1999.

Vlahakis, A., and Debnath, J. (2017). The interconnections between autophagy and integrin-mediated cell adhesion. J. Mol. Biol. *429*, 515–530. https://doi.org/10.1016/j.jmb.2016.11.027.

Wang, H., Liu, Y., Wang, D., Xu, Y., Dong, R., Yang, Y., Lv, Q., Chen, X., and Zhang, Z. (2019a). The upstream pathway of mTOR-mediated autophagy in liver diseases. Cells *8*, E1597. https://doi.org/10.3390/cells8121597.

Wang, R., Zhu, Y., Zhao, J., Ren, C., Li, P., Chen, H., Jin, M., and Zhou, H. (2019b). Autophagy promotes replication of influenza A virus in vitro. J. Virol. *93*. https://doi.org/10.1128/JVI.01984-18.

Woo, P.C.Y., Lau, S.K.P., Yip, C.C.Y., Huang, Y., Tsoi, H.W., Chan, K.H., and Yuen, K.Y. (2006). Comparative analysis of 22 coronavirus HKU1 genomes reveals a novel genotype and evidence of natural recombination in coronavirus HKU1. J. Virol. *80*, 7136–7145. https://doi.org/10.1128/JVI.00509-06.

Yang, B., Xue, Q., Guo, J., Wang, X., Zhang, Y., Guo, K., Li, W., Chen, S., Xue, T., Qi, X., and Wang, J. (2020). Autophagy induction by the pathogen receptor NECTIN4 and sustained autophagy contribute to peste des petits

ruminants virus infectivity. Autophagy *16*, 842–861. https://doi.org/10.1080/15548627.2019.1643184.

Yang, Y.L., Liang, Q.Z., Xu, S.Y., Mazing, E., Xu, G.H., Peng, L., Qin, P., Wang, B., and Huang, Y.W. (2019a). Characterization of a novel bat-HKU2-like swine enteric alphacoronavirus (SeACoV) infection in cultured cells and development of a SeACoV infectious clone. Virology *536*, 110–118. https://doi.org/10.1016/j.virol.2019.08.006.

Yang, Y.L., Qin, P., Wang, B., Liu, Y., Xu, G.H., Peng, L., Zhou, J., Zhu, S.J., and Huang, Y.W. (2019b). Broad cross-species infection of cultured cells by bat HKU2-related swine acute diarrhea syndrome coronavirus and identification of its replication in murine dendritic cells in vivo highlight its potential for diverse interspecies transmission. J. Virol. *93*. https://doi.org/10.1128/JVI.01448-19.

Yang, Z., and Klionsky, D.J. (2009). An overview of the molecular mechanism of autophagy. Curr. Top. Microbiol. Immunol. *335*, 1–32. https://doi.org/10.1007/978-3-642-00302-8_1.

Zeng, S., Peng, O., Sun, R., Xu, Q., Hu, F., Zhao, Y., Xue, C., Cao, Y., and Zhang, H. (2021). Transcriptional landscape of Vero E6 cells during early swine acute diarrhea syndrome coronavirus infection. Viruses *13*. https://doi.org/10.3390/v13040674.

Zhang, H., Cui, X., Cao, A., Li, X., and Li, L. (2020). ITGA3 interacts with VASP to regulate stemness and epithelial-mesenchymal transition of breast cancer cells. Gene *734*, 144396. https://doi.org/10.1016/j.gene.2020.144396.

Zhou, P., Fan, H., Lan, T., Yang, X.L., Shi, W.F., Zhang, W., Zhu, Y., Zhang, Y.W., Xie, Q.M., Mani, S., et al. (2018). Fatal swine acute diarrhoea syndrome caused by an HKU2-related coronavirus of bat origin. Nature *556*, 255–258. https://doi.org/10.1038/s41586-018-0010-9.

Zhou, P., Yang, X.L., Wang, X.G., Hu, B., Zhang, L., Zhang, W., Si, H.R., Zhu, Y., Li, B., Huang, C.L., et al. (2020). A pneumonia outbreak associated with a new coronavirus of probable bat origin. Nature *579*, 270–273. https://doi.org/10.1038/s41586-020-2012-7.

Zhu, L., Mou, C., Yang, X., Lin, J., and Yang, Q. (2016). Mitophagy in TGEV infection counteracts oxidative stress and apoptosis. Oncotarget *7*, 27122–27141. https://doi.org/10.18632/oncotarget.8345.

Zhu, Y., Li, L., Gong, S., Yu, Y., Dai, H., Cai, G., and Yan, J. (2015). ss3-integrin inhibits lipopolysaccharide-induced autophagy in cardiomyocytes via the Akt signaling pathway. Cardiology *130*, 249–259. https://doi.org/10.1159/000371489.

STAR★METHODS

KEY RESOURCES TABLE

REAGENT or RESOURCE	SOURCE	IDENTIFIER
Antibodies		
LC3B Rabbit mAb	CST	3868S
Akt Antibody	CST	9272
Phospho-Akt (Ser473) Rabbit Antibody	CST	9271
mTOR Antibody	CST	2972
Phospho-mTOR (Ser2448) Rabbit mAb	CST	5536
Anti-SQSTM1/p62 antibody	Abcam	ab101266
Anti-APG5L/ATG5 Antibody	Abcam	ab108327
HA Tag Polyclonal Antibody	Proteintech	51064-2-AP
GAPDH Monoclonal Antibody	Proteintech	60004-1-Ig
Integrin Alpha 3 Monoclonal Antibody	Proteintech	66070-1-Ig
HRP-conjugated Affinipure Goat Anti-Mouse IgG(H + L)	Proteintech	SA00001-1
HRP-conjugated Affinipure Goat Anti-Rabbit IgG(H + L)	Proteintech	SA00001-2
Anti-SADS-CoV-N Antibody	Prof. Yongchang Cao	N/A
Goat anti-Rabbit IgG (H + L) Highly Cross-Adsorbed Secondary Antibody, Alexa Fluor 488	Invitrogen	A-11034
Goat anti-Mouse IgG (H + L) Highly Cross-Adsorbed Secondary Antibody, Alexa Fluor 647	Invitrogen	A-21236
Bacterial and virus strains		
SADS-CoV strain GDS04	Prof. Yongchang Cao	N/A
PEDV strain GDS01	Prof. Yongchang Cao	N/A
Chemicals, peptides, and recombinant proteins		
Rapamycin	Sigma-Aldrich	V900930
3-MA	Sigma-Aldrich	M9281
bafilomycin A1	Selleckchem	S1413
Neferine	Selleckchem	S5144
MK2206	Selleckchem	S1078
Critical commercial assays		
jetPRIME®	Polyplus	101000046
Cell Counting Kit(CCK-8)	YEASEN	40203ES60
Deposited data		
The proteome data	This manuscript	PXD030559(EMBL-EBI)
Experimental models: Cell lines		
Vero E6	ATCC	CCL-81
IPI-FX	Prof. Shaobo Xiao	N/A
Oligonucleotides		
ATG5 RNAi 5′-GGCAUUAUCCAAUUGGUUU-3′	RiboBio	N/A
ATG5 RNAi 5′-GCAGAACCAUACUAUUUGC-3′	RiboBio	N/A
ITGA3 siRNA 5′-CAGGAUGGAUUUCAGGAUAUU-3′	GenePharma	N/A
ITGA3 siRNA 5′-AGAUGGAUGUAGAUGAGAACU-3′	GenePharma	N/A
ITGA3 siRNA 5′-CCUACAACUGGAAAGGAAACA-3′	GenePharma	N/A

(*Continued on next page*)

Continued

REAGENT or RESOURCE	SOURCE	IDENTIFIER
Akt siRNA 5′-GCUACUUCCUCCUCAAGAAUG-3′	GenePharma	N/A
Akt siRNA 5′-AAUGAAAGUGCCAUCAUUCUU-3′	GenePharma	N/A
Akt siRNA 5′-CGAGUUUGAGUACCUGAAGCU-3′	GenePharma	N/A
Software and algorithms		
GraphPad Prism8	GraphPad	https://www.graphpad.com
STRING (11.5)	STRING Consortium	https://cn.string-db.org/
Cytoscape (3.9.0)	Cytoscape Consortium	https://cytoscape.org/
cytoHubba (0.1)	cytoHubba	https://apps.cytoscape.org/apps/cytohubba

RESOURCE AVAILABILITY

Lead contact

Further information and requests for resources and reagents should be directed to and will be fulfilled by the lead contact, Hao Zhang (zhanghao5@mail.sysu.edu.cn).

Materials availability

This study did not generate new unique reagents.

Data and code availability

- The proteome data have been deposited at European Molecular Biology Laboratory- European Bioinformatics Institute (EMBL-EBI) and are publicly available as of the date of publication. Accession numbers are listed in the key resources table. All data reported in this paper will be shared by the lead contact, Hao Zhang (zhanghao5@mail.sysu.edu.cn), upon request.
- This paper does not report original code.
- Any additional information required to reanalyze the data reported in this paper is available from the lead contact, Hao Zhang (zhanghao5@mail.sysu.edu.cn), upon request.

EXPERIMENTAL MODEL AND SUBJECT DETAILS

Cells and viruses

The African green monkey kidney (Vero E6) was obtained from ATCC (ATCC number: CCL-81) (USA), and porcine ileum epithelial cell line (IPI-FX) was kindly provided by Professor Shaobo Xiao (Huazhong Agricultural University, Wuhan, China). All cells were cultured in Dulbecco's Modified Eagle Medium (DMEM) supplemented with 10% fetal bovine serum (FBS, Gibco) at 37°C with 5% CO_2. SADS-CoV strain GDS04 and PEDV strain GDS01 were isolated and propagated in our laboratory, which were described by our previous studies. Viral titers were evaluated by 50% tissue culture infectious dose ($TCID_{50}$) analysis on Vero E6 cells. The inactivated virus was obtained by UV light irradiation for 1 h and the absence of virus infectivity was confirmed by qPCR and $TCID_{50}$.

METHOD DETAILS

Viral infection and drug treatment

Vero E6 cells and IPI-FX cells reaching approximately 80–90% confluence were infected with SADS-CoV and the inoculums were exchanged with serum-free DMEM containing EDTA-free trypsin (Gibco) after 1.5 h incubation. A single-cycle of infection takes approximately 4–6 h (Yang et al., 2019a). For drug treatment, cells were treated with autophagy regulators rapamycin (1 μg/mL for Vero E6 cells, 0.5 μg/mL for IPI-FX cells), 3-MA (0.25 mM for Vero E6 cells, 0.1 mM for IPI-FX cells) or bafilomycin A1 (1 μM), at 6 hpi, and treated with Akt regulators MK2206 (1 μM) or Neferine (5 μM) at 1.5 hpi.

Plasmids and siRNAs

The monkey ITGA3 gene was amplified by reverse transcription (RT)-PCR from total RNA extracted of Vero E6 cells using gene-specific primers and cloned into pcDNA3.1(+) vector containing a C-terminal HA tag.

The plasmid was sequenced to confirm that the amplified products had no errors introduced by PCR amplification. RNA interference (RNAi) oligonucleotide 5′-GGCAUUAUCCAAUUGGUUU-3′, 5′-GCAGAACCA UACUAUUUGC-3′ were used for the ATG5 (L-004374-00-0005), 5′-CAGGAUGGAUUUCAGGAUAUU-3′, 5′-AGAUGGAUGUAGAUGAGAACU-3′, 5′-CCUACAACUGGAAAGGAAACA-3′ were used for the ITGA3, 5′-GCUACUUCCUCCUCAAGAAUG-3′, 5′-AAUGAAAGUGCCAUCAUUCUU-3′, 5′-CGAGUUUGAGUACC UGAAGCU-3′ were used for the Akt siRNA experiments. Vero E6 cells were transfected with plasmids or siRNAs using Jet Prime according to the manufacturer's instructions.

Western blotting

Cells were collected and lysed in lysis buffer (Beyotime) containing protease inhibitor cocktail (Medchem Express) for 30 min. The lysates were centrifuged at 12,000 g for 5 min and the supernatants were mixed with sodium dodecyl sulfate (SDS) loading buffer and then boiled for 5 min. The samples were run on an SDS-PAGE gel and transferred onto polyvinylidene fluoride (PVDF) membranes (Millipore, 0.2 μm). After blocking with 5% non-fat milk (Sangon Biotech, Shanghai) or 4% bovine serum albumin (BSA, Solarbio) for 1 h, the membranes were incubated with the primary antibody at 4°C overnight. Following three times washing using Tris-buffered saline with Tween-20 (TBST), the membranes were incubated with the corresponding secondary antibody for 1 h. Finally, the specific protein bands were detected and visualized using a blot scanner.

Confocal immunofluorescence microscopy

Vero E6 cells were grown on the glass bottom cell culture dish (15 mm, NEST) and infected with SADS-CoV followed by different pharmacological treatment. At 24 hpi, cells were fixed with precooled 4% paraformaldehyde in phosphate-buffered saline (PBS) for 15 min and permeabilized with 0.5% Triton X-100 for 15 min. Then, cells were blocked in 4% BSA for 1 h and subsequently incubated with the corresponding primary antibody for 1 h at room temperature. After washing with PBS, the corresponding secondary antibody was incubated with the cells for 1 h at 37°C. Finally, the cells stained with 4′,6-diamidino-2-phenylindole (DAPI) for 5 min at room temperature and were observed under a confocal microscopy.

Transmission electron microscopy

Vero E6 cells and IPI-FX cells were mock infected or infected with SADS-CoV and collected in the bottom of 1.5 mL Eppendorf tubes by centrifugation at 4000 *g* for 5 min at 24 hpi. Then the cell pellets were fixed in 2.5% glutaraldehyde diluted with PBS and next made into ultrathin sections. Finally, transmission electron microscope was used for observation.

Cell viability assay

Cell viability assay was determined by a cell counting kit (CCK8, YEASEN). Briefly, Vero E6 cells and IPI-FX cells were cultured in 96-well plates and allowed to grow overnight. Next, cells were treated with different pharmacological regulators for 24 and 36 hpi. CCK-8 reagent was subsequently added into cells for 1–4 h at 37°C according to the manufacturer's protocol. The absorption value was measured at 450 nm (OD_{450}) and the results were calculated compared to those for control cells.

Proteomic assay

Vero E6 cells were mock infected or infected with SADS-CoV at an MOI of 0.1. After 1.5 h of viral uptake, cells were collected and lysed at 24 hpi. Then, all proteins were digested into peptides and aliquots were detected by mass spectrometry (MS) to determine changes in protein abundance during SADS-CoV infection. A data-independent acquisition (DIA) approach was used for the MS acquisitions. All conditions were carried out in biological triplicate.

KEGG pathway enrichment was performed in Kyoto Encyclopedia of Genes and Genomes database (Kanehisa et al., 2021). Proteins involved in PI3K/Akt pathways were used to search protein-protein interaction network with "Multiple proteins" function in String online tool (version 11.0, accessed date: 04, 23, 2021) (Szklarczyk et al., 2021). Meaning of network edges was set to "confidence", and other parameters were set to default. The output result was downloaded as a short tabular text file for further analysis. Hub gene rank scores were calculated with Cytoscape app cytoHubba (v0.1) (Chin et al., 2014), and then visualized in Cytoscape (v3.9.0) (Shannon et al., 2003).

QUANTIFICATION AND STATISTICAL ANALYSIS

All experiments were conducted independently at least three times. Statistical analysis was performed using GraphPad Prism8 software and data were expressed as means ± standard deviations (SD). The significance of the differences between the two groups was determined by an unpaired two-tailed Student's t-test.